The Curved Wall Jet over a Circular Cylinder before the Interaction of Two Opposing Curved Wall Jets

H. S. Rew* and S. O. Park**

(Received June 3, 1995)

A curved wall jet before the interaction of two identical curved wall jets over a circular cylinder was investigated experimentally. Using hot-wire anemometry, the mean velocity, Reynolds stresses, and high order moments of the fluctuating velocity were measured. The turbulent kinetic energy and shear stress budgets were evaluated using the measured data. The correlation coefficient, $\overline{uv}/u'v'$, the normal stress ratio, $\overline{v^2}/\overline{u^2}$, and the principal direction of the Reynolds stress are presented. The effects of curvature and adverse pressure gradient on these diistributions are also discurssed. The turbulent kinetic energy and shear stress budgets in two regions before the interaction are analyzed in detail to illuminate the effect of the adverse pressure gradient on the turbulent transport.

Key Words: Correlation Coefficient, Normal Stress Ratio, Turbulent Kinetic Energy Budget, Shear Stress Budget

Nomenclature

h : Slot height of the wall jet, 10 mm
k : Turbulent kinetic energy
p : Fluctuating pressure
P, Pa : Static and atmospheric pressure, respectively
r : Radial distance from the cylinder surface
$r_{1/2}$: Radial distance from the cylinder, where $U = Um/2$
R : Radius of curvature of the cylinder, 100mm
s : Distance along the cylinder surface from exit
U : Streamwise mean velocity
Um : Maximum velocity of the curved wall jet
Uo : Exit mean velocity
$\overline{u_iu_j}$: Reynolds stress
$\overline{u_iu_ju_k}$: Triple moment
α_p : Principal direction of the Reynolds tensor
ε : Turbulent kinetic energy dissipation rate
V : Radial mean velocity
ρ : Fluid density
$'$: Rms. value
$\overline{\ }$: Time average

* Living System Reseach Laboratory LG Electronics Inc.
** Dept. of Aerospace Engineering, Korea Advanced Institute of Science and Technology.

1. Introduction

The effect of a surface curvature on the development of a two-dimensional wall jet has been studied by the requirement of the aeronautical industry, and by the interest in the emerging field fo fluidics in which bistable curved wall jet is important to fluidic element design. Experimental results for the flow direction on the cylinder surface which is not only tangential to the jet but also penetrating to it were discussed by Gertsen in the first European Mechanism Colloquium. (Wille and Fernholz, 1965) Gertsen found that the pressure distribution around the cylinder is strongly dependent on the ratio of the radius of cylinder and the slot height, and blowing condition. Previous studies on the single curved wall jet

developing along the circular cylinder (Alcaraz et. al. 1977; Dakos et. al. 1984; Wilson and Goldstein 1976) revealed that the turbulent motion is signifcantily affected by the surface curvature. Especially, Alcaraz et. al. studied the Reynolds stress transport phenomena and the interaction between the stable inner layer and the unstable outer layer using conditional sampling technique.

The interaction of two separate jets is a fundamental problem often associated with high lift airfoils, fluidic devices and other industrial flows where the turbulent mixing and coalescence of two turbulent shear layers are involved. Understanding of the physical process of this flow phenomena is important in the sense that it constitutes a typical problem of complex turbulent shear layer interaction. Previous studies (Gilbert 1988; Kind and Suthanthiran 1973; Lee and Chung 1983; Rew and Park 1988) on the wall jet-wall jet interaction revealed that the velocity profiles of the merged jet were very similar to those of conventional plane jets and the merged jet spread more rapidly than the conventional one. To help understand the flow situation, a schematic sketch is provided in Fig. 1. Two identical wall jets issus tangentially on a crircular cylinder surface from each slot. They initially develop as two curved wall jets along the cylindrical surface, and these two opposite jets collide near the centerline of the merged jet. The static wall pressure rises substantially high above the ambient pressure. Then, the wall jets detach from the surface because of this high pressure and are coalesced into a single free jet. This single jet is gradually developed to attain similarity. The mean and fluctuating velocity properties of this single jet were intensively described in our previous publication. (Park and Rew 1991, 1992; Rew and park 1993a) The difference among the single wall jets (Alcaraz et. al., 1977; Dakos et. al., 1984; Wilson and Goldstein 1976) and the present wall jet as shown in Fig. 1 are the distance between the exit and the detachment point and the ratio of h and R.

Using an I-probe, Rew and Park (1988) found that the inner layer velocity profiles of the curved

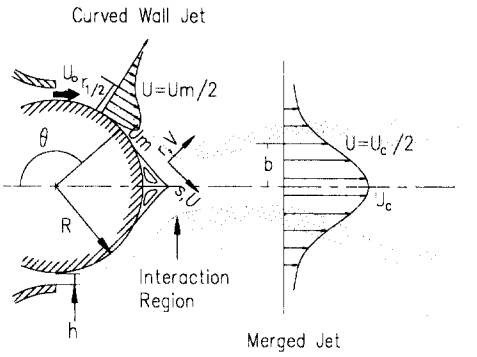

Fig. 1 Schematic of the flow configuration and coordinate system

wall jet with/without interaction show the logarithmic layes. However, the previous study focused only on the mean velocity profiles and turbulent intensity of the streamwise velocity component. For more thorough understanding of the turbulent flow features, especially of the curved wall jet before the interaction, additional measurements of turbulent structure quantities and its transport phenomena other than turbulent intensity would be necessary. In this study we attempt to carry out such additional measurements, which might produce the baseline data set for the curved wall jet interacting with upcoming opposite curved wall jet. Because the hot-wire anemometry cannot be used in the reverse flow region, the flow measurement near the separation region is excluded. The turbulent structural quantities, the Reynolds stress budgets of the curved wall jet will be included in this study.

2. Experimental set up and Measurements

The wind tunnel was symmetrically divided into two identical flow passages by vertical wall. Each flow passage consisted of a flow dividing section, a diffuser, a settling chamber and contraction ending with a slot. The contraction was composed of an inside circular cylinder and outer wall having the same radius of curvature as a circular cylinder (Fig. 1). The diameter was 200mm. The two slots at the end of the contraction were identical each other, each slot was

500mm deep. The slot height was 10mm, which gave a contraction ratio of 19 : 1 and an aspect ratio of 50 : 1. The exit velocity at each issuing slot was 29.2 m/sec, which gave the slot Reynolds number of 2.1×10^4. More details about the test rig can be found in Rew (1990) and the mean velocity and turbulent intensity at the slot can be found in Rew & Park (1993b). Static pressure taps were inserted into the central cylinder at every 2° for the portion of the cylindrical surface corresponding to the range $120°<\theta<240°$. (see Fig. 1) In this region, the pressure was expected to change rapidly. Elsewher, the taps were inserted at every 10°.

The mean velocity and Reynolds stree measurements were carried out using a DANTEC 55M CTA system equipped with 55P61 X-probe. (5μm tungsten wire) The overheat ratio was set at 0.8. The X-probe was calibrated for speed and yaw test was performed in the range of $-45°\sim+45°$. For the velocity calibration, a Pitot tube was connected to a Dywer micromanometer having a resolution of 0.013mm Aqa. The anemometer output was digitized by a Waveform Analyzer (DATA6000, Model 611, Data Precision Co.) equipped with a 14-bit A/D converter. The digitized hot-wire signals were converted into velocity using Bruun's formula. (1971) The sampling rate of fluctuating velocities was 20kHz. To compensate for the inaccuracy induced by the higt turbulence level, we adopted the correction method suggested by Müller. (1982)

3. Experimental Results and Discussion

3.1 Turbulent structure of the curved wall jet

As mentioned previously, the curved wall jets develop along the cylindrical surface. As well known, a wall jet possesses dual turbulent structure comprising the wall-layer turbulence and the free turbulence. These two turbulence structures interfere with each other. When the wall jet develops over a convex surface, the flow in the inner layer is stable and hence the turbulence activity is surpressed. On the other hand, in the outer free-jet like layer, the flow is unstable and the turbulence activity is thus enhanced. In this section, the data concerning turbulent structure are examined in detail.

Figure 2 shows a wall static pressure distribution along the cylindrical surface. When the wall jet leaves the slot and proceeds downstream, the pressure decreases further below the ambient pressure. When the two opposing wall jets start to interact, the pressure rises significantly high above the atmospheric pressure. The pressure distrbution along the cylindrical surface is symmetric about $\theta=180°$. The region of this symmetric 'pressure hump' may be viewed as a region of strong interaction of two opposing wall jets. The presence of separation bubble was confirmed by flow visualization. We found that the flow detachment occurred where the static pressure of the cylindrical surface was equal to the atmospheric pressure. (see Fig. 3)

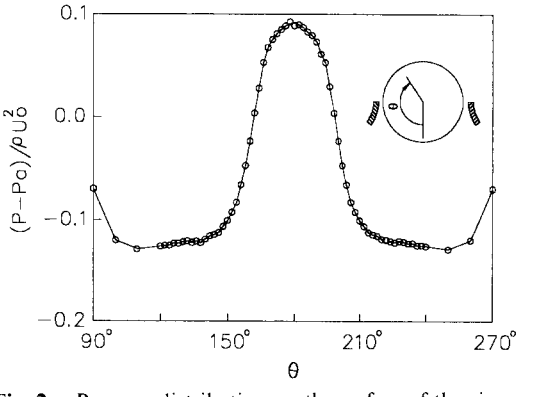

Fig. 2 Pressure distribution on the surface of the circular cylinder

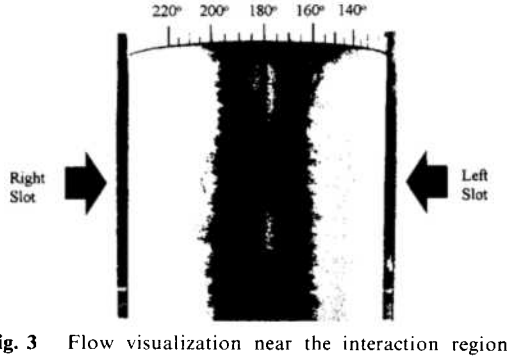

Fig. 3 Flow visualization near the interaction region using a black ink spray

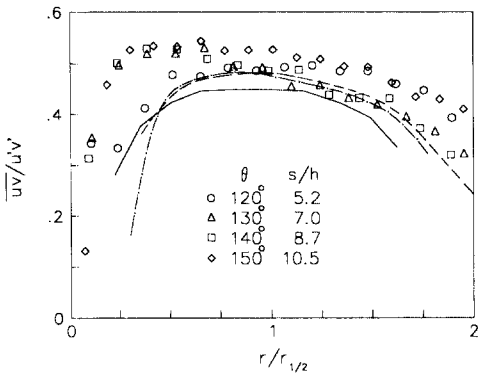

Fig. 4 Correlation coefficients of the curved wall jet; ——— Alcaraz et. al. (1977), ····· Dakos et. al. (1984), —·—· Irwin (1973)

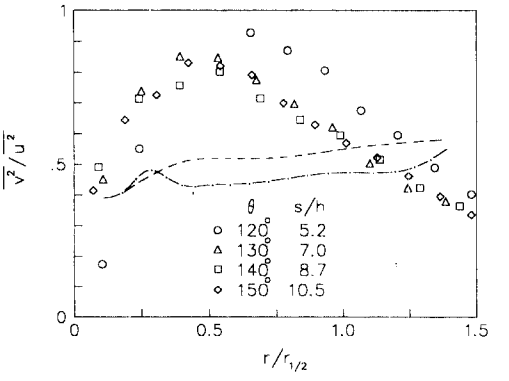

Fig. 5 Ratio of streamwise and radial velocity fluctuation of the curved wall jet; ····· Dakos et. al. (1984); —·—· Irwin (1973)

In a shear layer, a local equilibrium state of turbulent structure can be characteized by a constant value of the correlation coefficient, $\overline{uv}/u'v'$. Figure 4 displays the correlation coefficient distributions for the present case at various streamwise locations and those of other measurements for the plane and curved wall jets. The present correlation coefficient is about 0.5 for $0.5<r/r_{1/2}<1.5$. The corresponding coefficients for the curved wall jets of Alcaraz et. al. (1977) and of Dakos et. al. (1984) were 0.45 and 0.48, respectively. Irwin's coefficient for the plane wall jet (1973) under the adverse pressure gradient was about 0.48. Figure 4 shows that the present values of the correlation coefficient are, in general, higher than those of the other cases. A mild adverse pressure gradient does not significantly affect the correlation coefficient. Thus we believe that the hight correlation coefficient must have been caused by the smaller radius of curvature of the present geometry. The radii of curvature of Alcaraz et. al. and Dakos et. al. were larger by an order of magnitude than the present case.

In the study of a low Reynolds number turbulent boundary layer, Murlis et. al. (1982) suggested that the ratio of normal stresses, $\overline{v^2}/\overline{u^2}$, was a crude measure of the efficiency of turbulent mixing or the coherence of turbulent eddies and the ratio depended on the Reynolds number. The ratio of normal stresses for the present curved wall jet is plotted in Fig. 5 together with those for

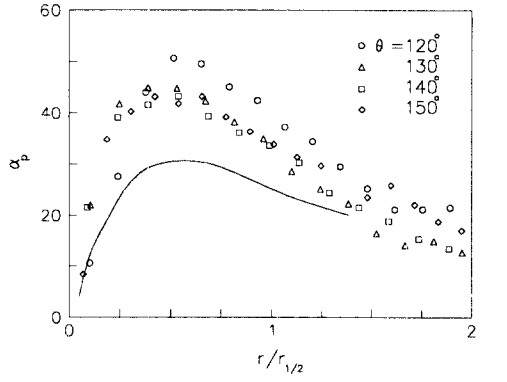

Fig. 6 Principal directions of the Reynolds tensor of the curved wall jet; ——— Alcaraz et. al. (1977)

the Irwin's plane wall jet and Dakos et. al.'s curved wall jet. The differences among these are remarkable. It seems to us that the differences are mainly due to curvature. For the present case, $h/R=0.1$, and for the case of Dakos et. al. $h/R=0.004$. For the plane wall jet, $h/R=0$ obviously, Therefore, we find that the normal stress ratio increases as the radius of curvature decreases. In sense of Murlis et. al., this implies that the turbulent mixing will be effective when the radius of curvature decreases. Browne et. al. (1984) found that $\overline{v^2}/\overline{u^2}$ was a more sensitive parameter than the correlation coefficient in describing the turbulence structural variation in their study of a turbulent plane jet. Form the data of Figs. 4 and 5, we realized that their observation is also valid for the case of the turbulent wall jet.

It is interesting to compare the principal direction of the Reynolds tensor of the present wall jet with that of the single curved wall jet (Alcaraz et. al., 1977) :

$$\tan 2\alpha_p=\frac{2\overline{uv}}{(\overline{u}^2-\overline{v}^2)} \tag{1}$$

Figure 6 displays the principal direction distributions for present case at various streamwise locations and that of other meausrement for the single curved wall jet. (Alcaraz et. al., 1977) As discernible in Fig. 6, the present α_p is much larger than that of Alcaraz et. al.'s wall jet. Considering pressure gradient in Fig. 2, a mild adverse pressure gradient does not significantly affect the principal direction of the Reynolds tensor. Thus we believe that the larger principal direction must have been caused by the smaller radius of curvature.

3.2 Reynolds stress transport in the curved wall jet

To understand the Reynolds stress transport phenomena in a complex turbulent flow, it is important to know how much each term contributes to its transport. Therefore, terms in the turbulent kinetic energy and shear stress equation were carefully evaluated. Neglecting the viscous diffusion term, the turbulent kinetic energy and share stress transport equations are as follows in cylindrical coordinate.

turbulent kinetic energy transport equation

$$\underbrace{U\frac{\partial k}{\partial s}+V\left(1+\frac{r}{R}\right)\frac{\partial k}{\partial r}}_{\text{i}}+\underbrace{\overline{u^2}\left(\frac{\partial U}{\partial s}+\frac{V}{R}\right)+\left(1+\frac{r}{R}\right)\overline{v^2}\frac{\partial V}{\partial r}+\overline{uv}\left(\left(1+\frac{r}{R}\right)\frac{\partial U}{\partial r}+\frac{\partial V}{\partial s}-\frac{U}{R}\right)}_{\text{ii}}$$
$$+\underbrace{\frac{\partial}{\partial s}\left(\frac{\overline{pu}}{r}\right)+\frac{\partial}{\partial r}\left(\left(1+\frac{r}{R}\right)\frac{\overline{pv}}{r}\right)}_{\text{iii}}+\underbrace{\frac{\partial}{\partial s}\overline{ku}+\frac{\partial}{\partial r}\left(\left(1+\frac{r}{R}\right)\overline{kv}\right)}_{\text{iv}}+\frac{\varepsilon}{v}=0 \tag{2}$$

shear stress transport equation

$$\underbrace{U\frac{\partial\overline{uv}}{\partial s}+V\left(1+\frac{r}{R}\right)\frac{\partial\overline{uv}}{\partial r}}_{\text{i}}+\underbrace{-\overline{u^2}\left(\frac{\partial U}{\partial s}-\frac{U}{R}\right)-\left(1+\frac{r}{R}\right)\overline{v^2}\frac{\partial U}{\partial r}+\frac{U}{R}(\overline{u^2}-\overline{v^2})}_{\text{ii}}$$
$$+\underbrace{-\frac{\partial}{\partial s}\left(\frac{\overline{pv}}{r}\right)-\left(1+\frac{r}{R}\right)\frac{\partial}{\partial r}\left(\frac{\overline{pu}}{r}\right)}_{\text{iii}}+\underbrace{-\frac{\partial}{\partial s}\overline{u^2v}-\left(1+\frac{r}{R}\right)\frac{\partial}{\partial r}(\overline{uv^2})-\frac{(2\overline{uv^2}-\overline{u^3})}{R}}_{\text{iv}}$$
$$+\underbrace{\frac{p}{r}\left(\frac{\partial v}{\partial s}+\left(1+\frac{r}{R}\right)\frac{\partial u}{\partial r}\right)}_{\text{vi}}=0 \tag{3}$$

Here, the i is the convection term, ii the production term, iii the pressure diffusion term, iv the velocity diffustion term, v in Eq. (2) the dissipation term, and vi in Eq. (3) the reditribution term. The terms i and ii and the velocity diffusion in Eqs. (2) and (3) were evaluated by central formula in radial direction using the measured data and their locations. The central difference or backward difference formula wew applied in the streamwise direction. However, the triple moments $\overline{uww}$ and $\overline{vww}$ in the turbulent kinetic energy equation was obtained using method discurssed by Azad et. al. (1987) For the dissipation term in Eq. (2), v, we adopted the isotropic turbulence and Taylor's frozen flow concept assumption. The terms in which pressure flucturation is involved will be hereinafter as the pressure transport term. As the pressure fluctuation could not be measured, we evaluated the pressure transport term by subtracting all measured terms from the balance.

Figure 7 shows the turbulent kinetic energy budget at $\theta=130°$. It should be noticed that the pressure gradient at $\theta=130°$ is small as shown in Fig. 2. The overall feature in Fig. 7 is similar to tat of Alcaraz et. al. From this budget, the pressure diffusion is far from being negligible, which shows a good agreement with the Alcaraz et al's result. As mentioned before, the curved wall jet over a convex wall possesses two turbulent struc-

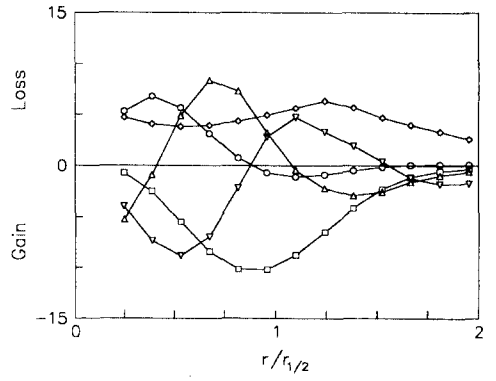

Fig. 7 Turbulent kinetic energy budget at $\theta=130°$; All termas are normalized by $r_{1/2}/Um^3\times10^3$; ○ convection; △ velocity diffusion; □ production; ◇ dissipation; ▽ pressure diffusion

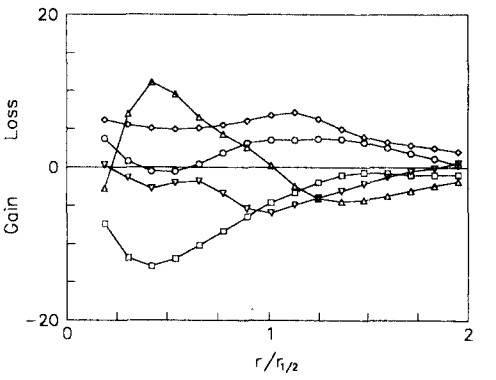

Fig. 9 Turbulent kinetic energy budget at $\theta=150°$; All terms are normalized by $r_{1/2}/Um^3\times10^3$; ○ convection; △ velocity diffution; □ production; ◇ dissipation; ▽ pressure diffutsion

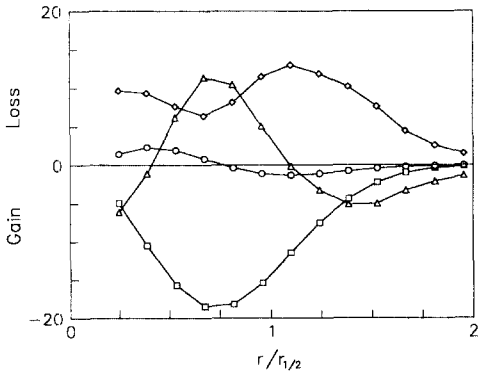

Fig. 8 Shear stress budget at $\theta=130°$; All terms are normalized by $r_{1/2}/Um^3\times10^3$; ○ convection; △ velocity diffusion; □ production; ▽ pressure transport

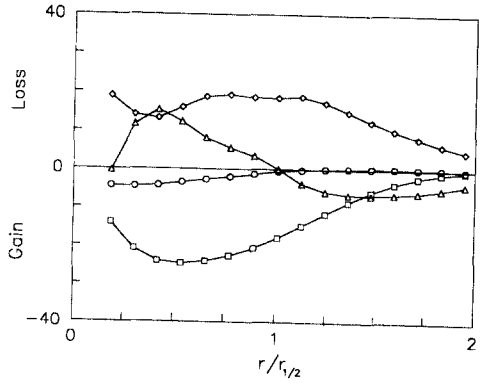

Fig. 10 Shear stress budget at $\theta=150°$; All terms are normalized by $r_{1/2}/Um^3\times10^3$; ○ convection; △ velocity diffusion; □ production; ▽ pressure transport

tures the turbulence activity is thus enhanced. Due to the active turbulent motion, the velocity diffuction plays an important role in turbulent kinetic energy transport as shown in Fig. 7. Also, the velocity diffusion distribution in Fig. 7 is much larger than that of a conventional plane jet. (Gutmark and Wygnanski, 1976). The shear stress plays an important role in the momentum transfer. The terms of the shear stress equation are plotted in Fig. 8. The production, velocity diffusion, and the pressure transport terms significantly contribute to the shear stress transport.

As mentioned previously, the pressure gradient at $\theta=150°$ is larger than that at $\theta=130°$. In previous study (Rew and Park, 1995), we found that the maximum shear stress position and zero crossing point of triple moment move to the wall as the wall jet developed along the curved wall. Therefore the maximum production position and the maximum diffusion positions are different from those at $\theta=130°$. The pressure diffustion distribution distnctly differs from that at $\theta=130°$ as shown in Fig. 9. The pressure diffusion is on gain side, which means that the turbulent kinetic energy comes from the pressure diffusion. The positive pressure diffusion was found in the strong interaction region where the two detached curved wall jets collide. (Park and Rew, 1992) It is known that the fluctuating pressure results from the eddy collision and fluctuating vorticity.

Therefore, we believe that the positive pressure diffusion results from the collision of the two detached wall jets. Figure 10 shows the terms in the shear stress tranport equation. The convection term in Figs. 8 and 10 are much samller than other terms. Clearly, the production, velocity diffusion, and the pressure transport terms in shear stress transport are most important, while the production and pressure transport terms are important in a conventional plane jet and the merged jet in the similar region. (Park and Rew, 1992).

4. Conclusions

A curved wall jet before the interaction of two opposite curved wall jets over a circular cylinder in still air was investigated experimentally. Using a hot-wire anemometry, the mean velocity and the Reynolds stress were measured and the turbulent structural quantities were analyzed in detail to illuminate the effects of the adverse pressure gradient and the radius curvature. The correlation coefficient of the present curved wall jet was about 0.5 for the range of $0.5 < r/r_{1/2} < 1.5$, which is somewhat larger than those of the wall jets with the larger radius of curvature. However, the ratio of normal stresses of the present curved wall jet was considerably larger than those of the previous wall jets having a large radius of curvature. From this observation, it can be concluded that the ratio of normal stresses is affected more sensitively by the curvature than by the correlation coefficient. Also, the principal direction of the Reynolds tensor of present case is larger than that of the curved wall jet having large radius curvature.

In the turbulent kinetic energy transport, the pressure diffusion is not negligible and the velocity diffusion plays an important role. Near the interaction region, the pressure diffusion is on gain side due to the eddy collision and fluctuating vorticity. The production, velocity diffusion, and the pressure transport terms significantly contribute to the shear stress transport.

References

Alcaraz, E., Charnay, G. and Mathieu, J., 1977, "Measurements in a Wall jet over a Convex Surface," *Phys. Fluids*, Vol. 20, pp. 203~210.

Azad, R. S., Kassab, S. G. and Dang, T. H., 1987, "Experimental Evaluation of Approximation for $\overline{w^2}$ and $\overline{vw^2}$," *AIAA J.*, Vol. 25, pp. 171~173.

Browne, L. B. W., Antonia, R. A. and Chambers, A. J., 1984, "The Interaction Region of Turbulent Plane Jet," *J. Fluid Mech.*, Vol. 149, pp. 353~373.

Bruun, H. H., 1971, "Linearization and Hot-wire Anemometry," *J. Phys. E.: J. Sci. Instrm.*, Vol. 4, pp. 815~820.

Dakos, T., Verriopoulos, C. A. and Gibson, M. M., 1984, "Turbulent Flow with Heat Transfer in Plane and Curved Wall Jets," *J. Fluid Mech.*, Vol. 145, pp. 339~360.

Gilbert, B. L., 1988, "Turbulence Measurements in a Two-Dimensional Upwash," *AIAA J.*, Vol. 26, pp. 10~14.

Gutmark, E. and Wygnanski, I., 1976, "The Planar Turbulent Jet," *J. Fluid Mech.*, Vol. 73, pp. 465~495.

Irwin, H. P. A. H., 1973, "Measurements in a Self-preserving Plane Wall Jet in a Positive Pressure Gradient," *J. Fluid Mech.*, Vol. 61, pp. 33~63.

Kind, R. J. and Suthanthiran, K., 1973, "The Interaction of Two Opposing Plane Wall Jets," *J. Fluid Mech.*, Vol. 58, pp. 389~402.

Lee, D. H. and Chung, M. K., 1983, "Interaction of a Pair of Curved Wall Jets after a Circular Cylinder," *AIAA Pap*, 83-0290.

Müller, U. R., 1982, "On the Accuracy of Turbulence Measurements with Inclined Hot Wires," *J. Fluid Mech*, Vol. 119, pp. 155~172.

Murlis, J., Tasi, H. M. and Bradshaw, P., 1982, "The Structure of Turbulent Boundary Layers at Low Reynolds Number," *J. Fluid Mech.*, Vol. 122, pp. 13~56.

Park, S. O. and Rew, H. S., 1991, "Turbulence Measurements in a Merged Jet from Two Opposing Curved Wall jets," *Exp. Fluids*, Vol. 10, pp. 241~250.

Park, S. O. and Rew, H. S., 1992, "Reynolds Stress Budget in the Outwash Jet Arising from Colliding Curved Wall Jets," *Exp. Thermal and*

Fluid Sci., Vol. 5, pp. 325~331.

Rew, H. S., 1990, "The Interaction of Two Curved Wall Jets over a Circular Cylinder," Ph. D. Thesis, KAIST.

Rew, H. S. and Park, S. O., 1988, "The Interaction of Two Opposing, Asymmetric Curved Wall Jets," *Exp. Fluids*, Vol. 6, pp. 243~252.

Rew, H. S. and Park, S. O., 1993, "Reynolds Stress Transport in a Merged Jet Arising from Two Opposing Curved Wall Jets," *KSME*, Vol. 17, pp. 416~425. (in Korean).

Rew, H. S. and Park, S. O., 1993, "Triple Moments and Their Transport in an Outwash Jet," *The 9th Turbulent Shear Flows*, Kyoto, Japan, Aug. 16~18, pp. 213.

Rew, H. S. and Park, S. O., 1995, "Turbulence Measurement in a Curved Wall Jet with Interaction," submitted to *J. KSASS* (in Korean)

Wille, R and Fernholz, H., 1965, "Report on the first European Mechanics Colloquium, on the Coanda Effect," *J. F. M.*, Vol. 23, pp. 801~819.

Wilson, D. J. and Goldstein, R. J., 1976, "Turbulence Wall Jets with Cylindrical Streamwise Surface Curvature," *J. Fluid Eng.*, Vol. 98, pp. 550~557.